THE JOURNAL OF PHYSICAL CHEMISTRY C
A JOURNAL OF THE AMERICAN CHEMICAL SOCIETY

pubs.acs.org/JPCC
Article

Unveiling the Spectroscopic Signatures of Poly(3,4-ethylenedioxythiophene) by Controlling Polaron and Bipolaron Concentrations

Rodrigo Rubio-Govea, Amanda Opis-Basilio, Adalid Torres, Mario Sánchez, Kallol Ray, and Katherine A. Mazzio*

Cite This: J. Phys. Chem. C 2024, 128, 18612−18621

Read Online

ACCESS | Metrics & More | Article Recommendations | Supporting Information

ABSTRACT: The electronic and optical properties of conductive polymers (CPs) are related to the formation of polarons and bipolarons localized along the polymer backbone. Their concentration is affected by the conformational and morphological features of the CPs, making it crucial to understand how they are affected by chain conformation and π-electron delocalization. In this work, we studied the modulation of the concentration of polarons and bipolarons in PEDOT:PSS after post-treatment with hydrazine and H_2SO_4, which influence the optical and electronic properties. Through a combination of electron spin resonance spectroscopy, UV−vis−NIR spectroscopy, Raman spectroscopy, and conductivity measurements, we evaluate changes in the properties of PEDOT, which are related to the chain conformation and π-electron delocalization within the polymer backbone. We present experimental evidence supporting the recently revised interpretation of the UV−vis−NIR spectrum of PEDOT:PSS, and through a combination of theoretical and experimental analysis, we propose a new interpretation of the Raman spectrum of PEDOT:PSS. Furthermore, we provide the first experimental evidence of the presence of polaron pairs in the triplet state in PEDOT:PSS, which have a spin of S = 1, which were only predicted theoretically up to this point.

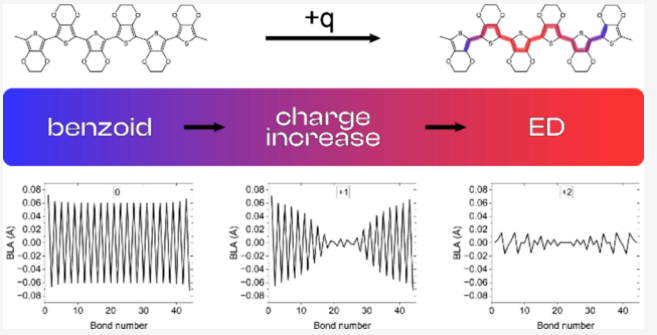

INTRODUCTION

The electronic and optical properties of conductive polymers (CPs) are related to the formation of polarons and bipolarons that represent single and double-charged quasiparticles, respectively, localized along the polymer backbone due to strong electron−phonon coupling.[1] In its pristine form (as-polymerized), the electrical conductivity (σ) of PEDOT:PSS is low (~1 S cm^{-1}).[2] However, its doping level can be tuned by chemical or electrochemical redox reactions (e.g., dimethyl sulfoxide or hydrazine (HZ) treatments), making it possible to modulate its σ. For instance, when it is post-treated with mineral acids (e.g., sulfuric acid (H_2SO_4)), it is possible to reach values close to 5,000 S cm^{-1}.[3] The high σ allows for its application in supercapacitors,[4] electrodes,[5] electrochemical transistors,[6] thermoelectrics,[7] sensors,[8] and photovoltaics,[9] among others. Similarly, it is also possible to improve the σ of PEDOT:PSS through secondary doping, which promotes the $\pi-\pi$ stacking of adjacent chains, leading to the formation of crystalline (lamellar) domains with extended percolation pathways, which improves charge carrier mobilities (μ).[10] On these grounds, it is crucial to understand how chemical treatments influence the chain conformation and π-electron delocalization and in turn, how this affects the optical and electronic properties of PEDOT. Elucidating the effects caused by post-treatments will provide a better understanding of how to modulate the properties of PEDOT, allowing for fine-tuning of processing techniques to provide the best results for its intended application.

Raman spectroscopy is a powerful characterization technique that can provide information about the structural arrangement of molecular systems and their chemical surroundings.[11] In the case of polyconjugated materials, Raman spectroscopy can give information regarding their structural order, long-range interactions, or confinement of π-electrons.[12] According to the effective conjugation coordination (ECC) theory postulated by Zerbi et al., the most significant Raman transitions in conjugated molecules are associated with the collective C═C/C−C stretching vibrations, referred to as Я modes.[13,14] Different works describe how the Я modes are affected by the effective conjugation

Received: August 20, 2024
Revised: October 7, 2024
Accepted: October 10, 2024
Published: October 18, 2024

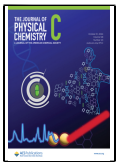

https://doi.org/10.1021/acs.jpcc.4c05602
J. Phys. Chem. C 2024, 128, 18612−18621

length (ECL) of the polymer chains.[15−18] As the π-conjugation increases, the C═C bonds are weakened and the C−C bonds are strengthened, causing a frequency downshift of the Я modes. Consequently, by comparing the frequency of the Я modes of the same polymer with different oxidation levels, it is possible to assign the most conjugated one to that having the lower frequency.[16] At the same time, when the oxidation level of PEDOT is varied, there is a concomitant evolution of its absorption spectra. Generally, undoped PEDOT shows an absorption peak at ∼600 nm, which is attributed to electronic transitions from the valence band (VB) to the conduction band (CB). As the oxidation (doping) level increases, there is an absorption peak that evolves between 700 and 1000 nm, which has been attributed to transitions from the VB to the CB of polaronic and bipolaronic states.[1] This is accompanied by the emergence of a peak at wavelengths >1500 nm, which has been attributed to transitions from the VB to empty polaronic and bipolaronic levels.[10] Upon further oxidation, the absorbance peak at ∼800−1000 nm reaches a maximum and then decreases, while the peak at wavelengths >1500 nm increases and becomes the dominant feature of the spectra.[19]

Electron spin resonance (ESR) spectroscopy can be used to determine the nature of the spins of the charge carriers present in PEDOT. Additionally, the signal obtained provides a spin count that can be used to determine the concentration of spin carriers. According to density functional theory (DFT) calculations, polaron signatures correspond to doublet states having a spin $S = 1/2$, while some bipolaronic states can promote the formation of polaron pairs corresponding to a triplet state having a spin $S = 1$.[1,19] The formation of the polaron pair is due to the increase of the π-conjugation which imparts a weakening of the double bonds. At the same time, as the number of thiophene rings in the quinoidal conformation is increased, the total potential energy gained by total aromatization also becomes greater. Together, the weakening of the double bond and the aromatic stabilization causes the existence of a number of rings for which the quinoidal closed-shell structure is unstable, promoting the cleavage of a double bond to become aromatic and form a polaron pair (biradical).[16] Once the polaron pairs are formed, the double-spin polarization (DSP) accounts for the π-conjugation of electrons in the doubly occupied orbitals into the singly occupied molecular orbitals, accounting for the triplet state.[20] Sahalianov et al. demonstrated through DFT calculations that in the case of polythiophenes, the singlet state is energetically higher than the triplet state,[19] supporting the notion of the presence of polaron pairs. However, up to this point, their presence has not been confirmed experimentally.

In this work, we modulate the concentration of polarons and bipolarons in PEDOT:PSS films through post-treatment with HZ and H_2SO_4, which can effectively reduce and oxidize the PEDOT films, respectively. After varying the oxidation levels by doping, changes in the optical and electronic properties are observed. We analyzed the modulation of polarons and bipolarons through a combination of ESR spectroscopy, UV−vis−NIR spectroscopy, Raman spectroscopy, and σ measurements. Our ESR measurements provide the first experimental evidence of the presence of polaron pairs in the triplet state in PEDOT:PSS, having a total spin $S = 1$. These results provide evidence that strongly supports the revised interpretation of the UV−vis−NIR spectrum of PEDOT:PSS proposed by Zozoulenko et al.[1] Additionally, through a combination of theoretical and experimental analysis, we propose a revised interpretation of the Raman spectrum of PEDOT:PSS, where we find that it is more pertinent to analyze and discuss it in terms of electron delocalization (ED) instead of the conformational change between quinoidal and benzoidal structures.

METHODOLOGY

Reagents. Acetonitrile, hydrazine (HZ), sulfuric acid (H_2SO_4), and isopropanol were procured from Sigma-Aldrich. Poly(3,4-ethylenedioxythiphene):poly(styrene sulfonic acid) (PEDOT:PSS, PH1000) was purchased from Ossila. All deionized (DI) water used was ultra pure (>18 MΩ cm). All materials were used as received unless otherwise noted.

Thin Film Fabrication. PEDOT:PSS was filtered with a 0.45 μm nylon syringe filter prior to deposition for all thin films. The films for the UV−vis−NIR and Raman characterization were prepared by depositing 200 μL of PEDOT:PSS onto 20 mm × 20 mm plasma-cleaned glass, afterward they were spin coated at 1k rpm for 60 s followed by annealing at 120 °C for 2 min. For the ESR measurements, 20 μL of PEDOT:PSS was deposited onto plasma-cleaned quartz substrates of approximately 10 mm × 4 mm and dried at 120 °C for 2 min. The films for the σ measurements were prepared by drop casting 40 μL of PEDOT:PSS onto thin film analyzer (TFA) chips and drying at 60 °C. After the complete evaporation of water, the temperature was raised to 120 °C and left to anneal for 5 min.

Thin Film Post-Treatment. For the HZ post-treatment, different HZ solutions with concentrations of 0.2, 0.4, 0.6, and 0.8 M, were prepared by adding different amounts of a 1 M HZ stock solution in acetonitrile to achieve the desired concentrations. Afterward, each sample was treated with 40 μL and left to react for 2 min, then the samples were rinsed with isopropanol and dried at 120 °C for 5 min. For the H_2SO_4 post-treatment, the 3.7, 7.4, 11, and 14.7 M solutions were prepared by diluting concentrated H_2SO_4 (18.4 M) with DI water. Afterward, each sample was treated with 40 μL and left to react for 2 min, then the samples were rinsed with isopropanol and dried at 120 °C for 5 min.

UV−vis−NIR Spectroscopy. UV−vis−NIR absorption measurements were performed on a Cary 5000 UV−vis−NIR spectrophotometer from Agilent. The spectra were recorded in the range from 300 to 2,500 nm, measuring with an interval of 1 nm and acquisition time of 1 s.

Raman Spectroscopy. Raman measurements were conducted using a Renishaw inVia confocal Raman microscope with a 785 nm laser. To prevent laser damage to the samples, the measurements were performed with 0.1% laser power and an exposure time of 60 s for 3 accumulations. The deconvolution of the Raman spectra was done using Origin 2019 software with a Lorentzian line shape without applying any constraints to the peak center and line width, i.e., full width at half-maximum (fwhm). The peak center was left without a position constraint since its position shifts depending on the effective conjugation length. In a similar manner, no constraint for the fwhm was used since its value changes as the crystallinity of the lamellar domains is modified, where a small fwhm corresponds to higher crystallinity of the lamellar domains, and vice versa.[21]

Electron Spin Resonance (ESR) Spectroscopy. Continuous wave (CW) X-band electron spin resonance spectra were collected on a Bruker EMXplus Instrument at a frequency of ∼9.64 GHz in perpendicular polarization and ∼9.38 GHz in

https://doi.org/10.1021/acs.jpcc.4c05602
J. Phys. Chem. C 2024, 128, 18612−18621

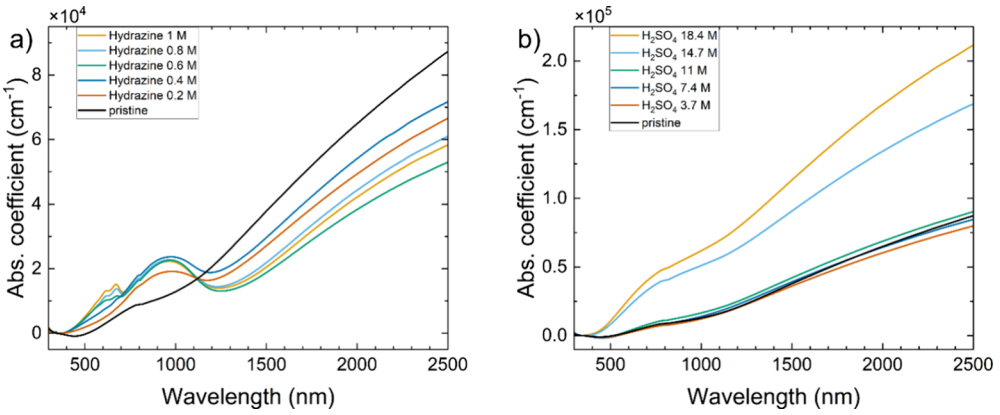

Figure 1. UV−vis−NIR spectrum of PEDOT:PSS treated with different concentrations of (a) hydrazine and (b) H_2SO_4.

parallel polarization using a dual-mode Bruker ER4116DM probehead. For low-temperature measurements, a liquid Helium cooling system, coupled to a cryostat, was used. Before inserting the samples in the resonator, they were placed inside an ESR quartz tube (4 mm) and then frozen in liquid nitrogen before measurement. They were measured in a range from 13 to 20 K. The empty quartz tube was measured as a blank, to demonstrate that none of the signals arise from it.

Electrical Conductivity (σ) Measurements. Conductivity measurements were performed on a Linseis TFA on test chips consisting of a four-contact van der Pauw measurement setup for the determination of the electrical transport properties.[22,23] All samples were subjected to two heating−cooling cycles between 20 and 120 °C. All properties were measured every 10 °C with a heating/cooling rate of 10 °C min^{-1}.

Density Functional Theory (DFT) Calculations. The geometry optimizations were accomplished using the Gaussian 16 package without imposing any constraints on initial structures.[24] Neutral PEDOT ($Q = 0$) and p-doped PEDOT ($Q = +1e, +2e, +3e, +4e$) were optimized using the ωB97x-D[25] functional with the 6-31G(d,p) basis set.[26] The length of the PEDOT oligomers (12 monomers) was chosen to keep consistency with other DFT calculations of PEDOT.[1,27] The ωB97x-D functional was chosen as it has been shown to accurately model molecular geometries, interaction energies, and electron delocalization for PEDOT:PSS systems.[27]

RESULTS

Ultraviolet−Visible−Near Infrared (UV−vis−NIR) spectroscopy. The most commonly employed method for following changes in the oxidation level of PEDOT is UV−vis−NIR spectroscopy, as it allows a qualitative determination of the majority of charge carriers (polarons or bipolarons) present in the structure.[1,28] Traditionally, the absorption spectrum of PEDOT:PSS was divided into three main regions, namely the neutral region (~500−650 nm), the polaronic region (~700−1200 nm), and the bipolaronic region (>1200 nm).[29] These bands were attributed to optical transitions from half-filled polaronic bands to the CB for polarons, and from the VB to empty bipolaronic levels for bipolarons. Nevertheless, Zozoulenko et al. showed through DFT calculations that the spectrum is more complex and that the "polaronic" and "bipolaronic" regions are composed of a mixture of polaronic and bipolaronic transitions that tend to overlap in the spectrum.[1] In this revised interpretation, the polaronic optical transitions correspond to transitions from the VB to empty polaronic bands and to the CB. Similarly, the bipolaronic optical transitions correspond to transitions from the VB to empty bipolaronic bands.

To follow the evolution of the UV−vis−NIR spectrum of PEDOT as its oxidation level is decreased, we post-treated the films with HZ.[30] As shown in Figure 1a, when PEDOT:PSS is treated with increasing concentrations of HZ, there is a concomitant increase in the absorption spectra in the regions around ~660 nm and ~960 nm and a decrease in the NIR region at wavelengths >1200 nm. These results follow the expected evolution of the absorption spectrum as the oxidation level of PEDOT:PSS is decreased.[29,30] On the other hand, to follow the evolution of the absorption spectrum as the oxidation level is increased, we post-treated the films with H_2SO_4. As shown in Figure 1b, when PEDOT:PSS is treated with increasing concentrations of H_2SO_4, there does not seem to be an apparent change in the absorption spectrum when concentrations ranging from 3.7 to 11 M were used. Nevertheless, there is a considerable increase in the absorption region of ~900 nm and >1200 nm when treated with concentrations higher than 14.7 M. This gives a first indication that the overall concentration of polarons/bipolarons is increasing.[31] To better describe the type of charge carriers (polarons and/or bipolarons) present in the treated samples, they were analyzed with ESR spectroscopy.

Electron Spin Resonance (ESR) Spectroscopy. We employed CW X-Band ESR spectroscopy to further investigate the nature of the charge carriers present in PEDOT:PSS samples after different post-treatments. As described by Zozoulenko et al.,[1] two types of spins can be detected by ESR. The first corresponds to the polaronic states (odd number of charges) corresponding to doublet states having a spin $S = 1/2$. The second one corresponds to bipolaronic states or polaron pairs having an effective charge of +2 and can have a total spin $S = 0$ or 1. For the case of $S = 0$, the state is spin-degenerate and describes what is called a bipolaron. For the case when $S = 1$, the spin degeneracy no longer exists and the state corresponds to a triplet state, more commonly known as polaron pair or biradical. It is important to identify the presence of polarons and/or bipolarons/polaron pairs in PEDOT films, as they can impact the transport properties.

The origin of the ESR signal of PEDOT:PSS is usually regarded to originate from polarons, and the reduction of its intensity is attributed to the formation of bipolarons that are not detected by the most common ESR technique employed

https://doi.org/10.1021/acs.jpcc.4c05602
J. Phys. Chem. C 2024, 128, 18612−18621

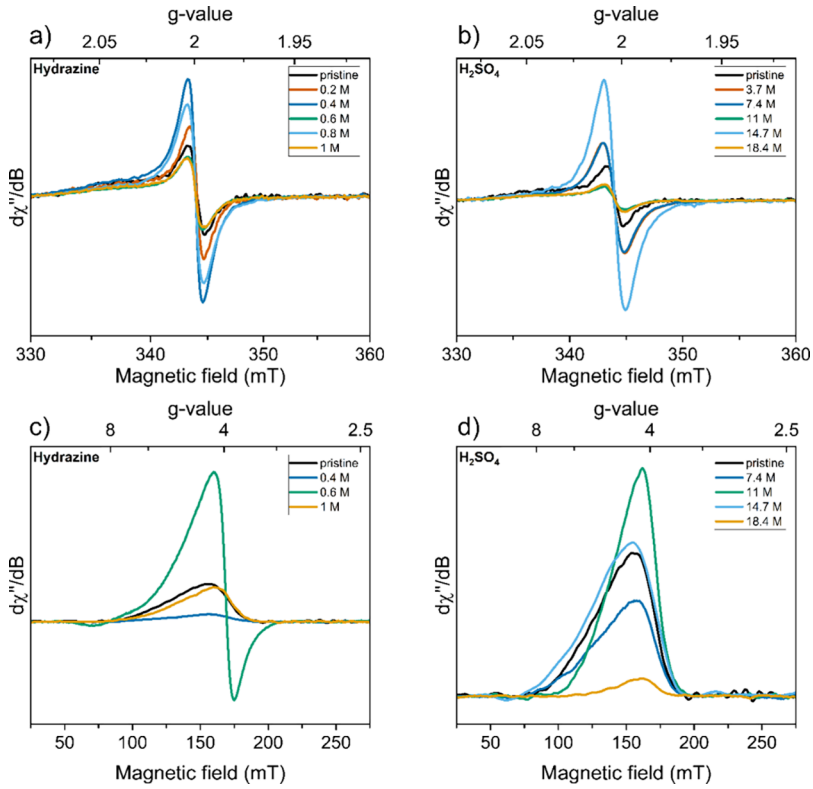

Figure 2. Room temperature ESR spectra of (a) HZ and (b) H_2SO_4 post-treated PEDOT:PSS samples. Low temperature ESR spectra of (c) HZ and (d) post-treated PEDOT:PSS samples.

(measurements in the perpendicular polarization CW-ESR, which allows detection of half-integer spin systems).[32] To follow changes in the polaron concentration of PEDOT:PSS films after post-treatment, we conducted measurements at room temperature. All the spectra were normalized to the sample weight to make it possible to compare changes in polaron concentration. As shown in Figure 2a, there is a decrease of the polaron signal relative to the pristine sample when post-treated with HZ concentrations of 0.6 and 1 M, suggesting a shift from polarons to bipolarons and/or polaron pairs. On the contrary, when post-treated with HZ concentrations of 0.2, 0.4, and 0.8 M, there was an increase in the signal intensity, suggesting an increase of the polaron concentration.[33] Similarly, as shown in Figure 2b, the samples post-treated with H_2SO_4 in concentrations of 3.7, 7.4, and 14.7 M present an increased concentration of polarons, and the samples post-treated with concentrations of 11 and 18.4 M show a decreased concentration of polarons. Nonetheless, all the samples present the typical ESR signal that is expected to arise from PEDOT:PSS samples, corresponding to polarons with spin $S = 1/2$ and a g-value around 2.00.[34,35] The g-values of all samples were calculated from resonance using eq 1:

$$g = \frac{h\nu}{\mu_B B} \tag{1}$$

where h is the Planck constant, ν is the microwave frequency, μ_B is the Bohr magneton, and B is the resonance magnetic field.[36] The obtained g-values for all samples are presented in Table S1.

In an attempt to detect polaron pairs in a triplet state with $S = 1$, we employed measurements using parallel polarization CW-ESR. This is a useful technique to observe ESR spectra of integer spin systems due to the possibility to record transitions with $\Delta m_s = \pm 2$. Low temperature (~13−20 K) was employed in the parallel-mode measurements to enhance the chances of seeing the above-mentioned transitions, as it is known that low-temperature measurements facilitate the detection of electron spins that present fast relaxation times.[37] Additionally, the signal from triplet states is greatly enhanced when the microwave radiation is applied parallel to the magnetic field, due to selection rules.[38] As shown in Figure 2c,d, all of the measured samples in the ESR parallel mode present a signal between 155 and 160 mT, and we posit the possibility that this signal corresponds to polaron pairs in a triplet state having $S = 1$. The corresponding g-values are presented in Table S1. These results are in agreement with the predictions made by Zozoulenko et al. through DFT calculations of the presence of triplet states with $S = 1$ in polythiophene systems.[1,19] These results will be further addressed in the discussion section. Also, it is possible to see that, depending on the treatment employed, there is no complete conversion between polarons and bipolarons, as some of the samples measured in the parallel polarization showed signals around $g \approx 4$, corresponding to the triplet state, together with the signal around $g = 2$, corresponding to the doublet state, as shown in Figure S1. These results agree with the DFT calculations done by Sahalianov et al., where they predict the coexistence of polarons and bipolarons within the same oligomers.[19]

Raman Spectroscopy. The main symmetric $C_\alpha{=}C_\beta$ stretching band of PEDOT:PSS is composed of different contributions of the collective vibrations of PEDOT chains with different effective conjugation lengths (ECLs). Generally, vibrational modes related to short ECLs tend to appear at approximately 1450 cm^{-1} and as the ECL is increased, the vibrations downshift.[39−41] The mixture of different ECLs that

https://doi.org/10.1021/acs.jpcc.4c05602
J. Phys. Chem. C 2024, 128, 18612−18621

gives rise to the main symmetric C_α=C_β peak can be correlated to the charge carrier mobility (μ) of the samples. It has been reported for different polythiophene systems that the ECL and position of the symmetric C_α=C_β peak are related to the chemical structure of the thiophene backbone.[18,42]

As the neutral thiophene is oxidized into a polaron, the thiophene oligomer tends to shift from a benzoidal to a quinodal conformation. As it is further oxidized, the formation of a bipolaron (polaron pair) is promoted, resulting in a full quinoidization of the thienyl backbone due to the strong electrostatic repulsion between the positive charges confined in a relatively small molecule.[40,42,43] By deconvoluting the main symmetric C_α=C_β stretching band of the pristine and post-treated PEDOT:PSS, it is possible to estimate if the stretching band is composed of one or more ECLs, with the number of deconvoluted peaks corresponding to the number of ECLs in the polymer domain. At the same time, the fwhm of the deconvoluted peaks indicates the crystallinity of the domains,[21] and the relative intensities reflect the contribution of each ECL to the whole. In our previous study,[44] we demonstrated the importance of determining the different contributions from the ECL that make up the main symmetric C_α=C_β stretching band and its role in modulating the μ of the samples, making it an important parameter when considering the modulation of σ.

Figure 3 shows an example of the deconvolution of the symmetric C_α=C_β peak of pristine PEDOT:PSS. From here it

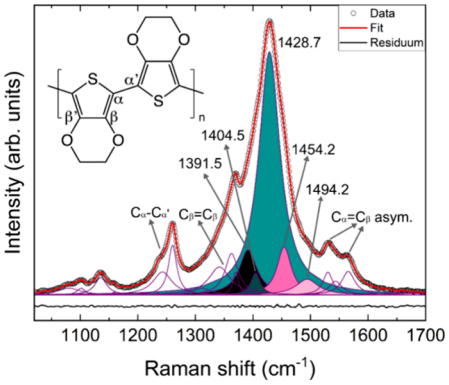

Figure 3. Deconvolution of the main C_α=C_β symmetric stretch of pristine PEDOT:PSS. The inset corresponds to the schematic representation of the chemical structure of PEDOT.

can be seen that the main vibrational mode can be deconvoluted into five different contributions centered at 1391.5, 1404.5, 1428.7, 1454.2, and 1494.2 cm^{-1}. From this, it is evident that the pristine PEDOT:PSS film consists of a mixture of different ECLs, having a considerable contribution of short ECLs located at higher wavenumbers.[41,45] In the same manner, the multiple contributions of the deconvoluted C_α=C_β asymmetric stretch, C_β=$C_{\beta'}$ stretch, and C_α=$C_{\alpha'}$ inter-ring stretching correspond to the same vibrational modes of different sections of the PEDOT chain, e.g., central and terminal thiophene rings, with different ECLs.[46] Figures showing the deconvoluted Raman spectra of all PEDOT:PSS samples treated with different concentrations of HZ and H_2SO_4 can be found in Figures S2 and S3, respectively, of the Supporting Information. The results from the deconvolution of the main symmetric C_α=C_β peak are summarized in Table S2 and addressed further in the discussion section.

DFT Simulation of the Raman Spectrum of PEDOT. Generally, the shifts observed in the Raman spectrum of PEDOT are attributed to a conformational change from the benzoid to the quinoid (aromatic) structure, Figure 4, with

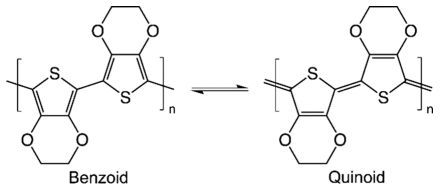

Figure 4. Schematic representation of the benzoid and quinoid chemical structures of PEDOT.

PEDOT being purely in one of the two conformations.[47−51] Also, while it is true that there is a conformational change as the oxidation level of PEDOT is varied, there is always a mixture of benzoid/quinoid conformations present in the PEDOT chain regardless of its oxidation level.[1,10]

To better understand the variation of the Raman spectrum of PEDOT as its oxidation level is varied, the Raman spectrum was simulated through DFT. It has been established that Raman spectroscopy is sensitive to the extent of electron delocalization (ED) along the conjugated backbone of polymers, as explained by the ECC.[18,46] According to the definition established by the IUPAC, ED is a quantum mechanical concept most usually applied in organic chemistry to describe the π-bonding in a conjugated system. This bonding is not localized between two atoms. Instead, each link has a "fractional double bond character" or bond order, and some degree of delocalization is always present and can be estimated by quantum mechanical calculations.[52]

To this end, the bond-length alternation (BLA) parameter can give direct information regarding the ED of the conjugated polymer. The BLA is defined as the average distance of consecutive single and double bonds in a π-delocalized system, see Figure 5a. A value of BLA of zero or close to zero indicates a high degree of aromaticity and ED. On the contrary, larger BLA values indicate electron localization and consequently, the absence of aromaticity.[16,18,53] Figure 5b−f shows the calculated BLA obtained from geometry-optimized PEDOT oligomers with charges 0, +1, +2, +3, and +4. From here, it can be seen that as the charge of PEDOT is increased, there are some regions of the BLA pattern that have values close to zero which can be assigned to the monomers where the charge is delocalized, and thus are present in the quinoid conformation. Kim and Zozoulenko, reported a similar behavior for PEDOT chains composed of 6, 9, and 12 oligomers, where the backbone adapts a quinoid conformation as the charge is increased.[54]

It has been established, through the ECC, that there is an accompanying redistribution of the C=C/C−C bonds as the π-conjugation is increased, causing a frequency downshift of the strongest Raman vibrational modes.[16] Because of this, it is possible to compare the strongest vibrational mode of the same oligomer with differing ED, i.e. the symmetric C_α=C_β stretching mode of PEDOT, where the vibrational frequency of the most conjugated molecule will appear at a lower value. Figure S4 shows the simulated Raman spectra of PEDOT with increasing net charge. From here, it can be seen that there is an expected increase in the number of vibrational modes in the Raman spectra as the charge on PEDOT is increased from 0 to

https://doi.org/10.1021/acs.jpcc.4c05602
J. Phys. Chem. C 2024, 128, 18612−18621

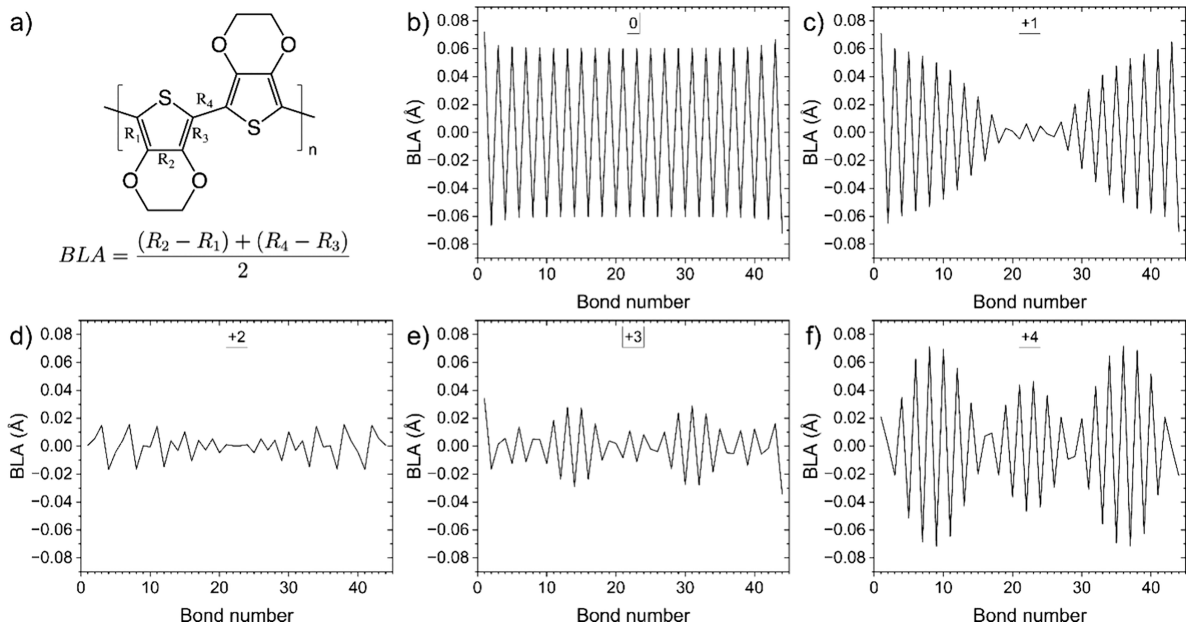

Figure 5. (a) Definition of the BLA in PEDOT. BLA calculated for PEDOT with charges of (b) 0, (c) +1, (d) +2, (e) +3, and (f) +4 obtained from the optimized molecular geometries.

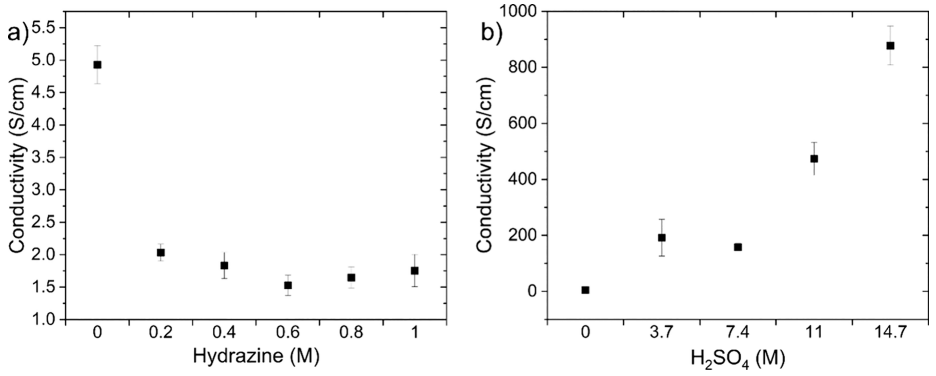

Figure 6. Conductivity of (a) HZ and (b) H_2SO_4 post-treated PEDOT:PSS samples at 20 °C.

+4. It is important to note that the calculated frequencies are expected to reflect the experimental values better than their corresponding intensities, and these can therefore be used to understand the trends observed experimentally.[16] By analyzing the region between 1400 and 1500 cm^{-1}, it is possible to assess the effect that increasing charge has on the $C_\alpha{=}C_\beta$ stretching mode. As the charge is increased from 0 to +3, there is a downshift of the main peak followed by an upshift when the charge is +4. This trend follows the evolution observed in Figure 5, where the BLA is reduced going from charge 0 to +3, and then it increases at charge +4.

We stipulate that the observed differences in the intensity between the experimental spectra and the simulated ones is due to the fact that the simulated spectra is calculated only from one chain when in reality the PEDOT:PSS films are composed of a mixture of amorphous and crystalline domains consisting of several $\pi{-}\pi$ stacked chains promoting an interchain coupling. It is known that the interchain coupling can lead to modifications of the polaronic/bipolaronic states, causing the stacked chains to present physical effects that would not be considered during the simulations.[1] In addition, we did not include the presence of counterions in our simulations, which are known to cause a strong localization of polarons/bipolarons in the PEDOT chain, which will also affect the intensity of the simulated spectra.[19] Nevertheless, this model represents a good starting point for the interpretation and understanding of how the morphological conformation of the PEDOT chains (benzoid/quinoid) affects observed shifts in the vibrational modes. As stated above, the vibrational frequency of the symmetric $C_\alpha{=}C_\beta$ stretching mode of PEDOT tends to downshift as the conjugation length is increased. Based on the results shown in Figure 5, the symmetric $C_\alpha{=}C_\beta$ stretching of $PEDOT^{2+}$ and $PEDOT^{3+}$ should appear at lower frequencies relative to those of other charge states, as they are the species with the lowest BLA values. The results presented in Figure S4 are in agreement with the expected shifts.

There is a common misconception in the PEDOT literature where observed Raman shifts are interpreted as being based on a complete transition from benzoid to quinoid conformations, and vice versa.[55−58] However, as shown in Figure 5, it is clear that the only case where the PEDOT chain is present in a single conformation (benzoid) is in its neutral state. For all the other cases where PEDOT has a charge, there are always mixtures of the benzoid/quinoid configuration. These results provide useful information regarding the assignment of the

https://doi.org/10.1021/acs.jpcc.4c05602
J. Phys. Chem. C 2024, 128, 18612−18621

observed shifts of the vibrational modes present in the charged PEDOT chains, making it clear that there is a need to revise the common interpretation of the Raman spectrum, where it is more pertinent to discuss it in terms of the ECL (ED) rather than the benzoid/quinoid conformation.

Electrical Conductivity (σ) Measurements. To evaluate the effect that the HZ and H_2SO_4 post-treatments have on the σ of PEDOT:PSS, each sample was evaluated by measuring two heating/cooling cycles between 20 and 120 °C. Figures S5 and S6 of the Supporting Information show the σ of PEDOT:PSS in its pristine state and after post-treatment with HZ and H_2SO_4, respectively. The reported error arises from a combination of measurement errors as reported by the instrument manufacturer alongside the thickness deviation of the sample as determined by profilometry, a full description of the error calculation can be found in the Supporting Information. As the σ of the samples only presents a small variation in the whole temperature range, the results presented in Figure 6a,b, and the following discussion, only report the values obtained at 20 °C.

As shown in Figure 6a, there is a 41% decrease in σ from the pristine PEDOT:PSS (4.93 ± 0.29) S cm^{-1} to that of the PEDOT:PSS post-treated with a 0.2 M HZ solution (2.03 ± 0.13) S cm^{-1}. However, there are only marginal differences in σ with increasing concentrations of HZ up to 1 M. The lowest σ (1.53 ± 0.16) S cm^{-1} is reached when post-treated with a 0.6 M HZ solution. In the case of the H_2SO_4 post-treatment, shown in Figure 6b, there is an increase in σ with increasing concentration of H_2SO_4, reaching its highest value of (877.88 ± 70.11) S cm^{-1} when post-treated with a concentration of 14.7 M H_2SO_4. Due to processing problems, it was not possible to measure the sample post-treated with 18.4 M H_2SO_4, see Figure S7 of the Supporting Information for further information. The increase of the σ after H_2SO_4 post-treatment is in agreement with the results reported by Kim et al.[59]

DISCUSSION

By analyzing the results obtained from the UV−vis−NIR absorption and the ESR spectra, it is possible to have a qualitative evaluation of how the UV−vis−NIR absorption spectra are modified by modulating the concentration of polaron/bipolarons (polaron pairs). As seen in Figure 1a, after the samples were treated with increasing concentrations of HZ, there is the expected evolution of the absorption peak at ∼660 nm corresponding to the neutral portion of PEDOT. In the same manner, there is a concomitant increase in the absorption at ∼960 nm. In the case of the H_2SO_4 post-treatment, shown in Figure 1b, all the samples show an increased absorption in the range between 700 and 900 nm and an increased absorption in the NIR region. Based on the revised interpretation of the absorption spectrum of PEDOT reported by Zozoulenko et al.,[1] the peak at ∼960 nm corresponds to the optical transition from the VB to empty polaronic/bipolaronic states and to the CB. The absorption in the NIR region corresponds to transitions from the VB to empty polaronic/bipolaronic states. As shown in the room temperature ESR results in Figure 2a,b, all the samples show the expected signal corresponding to polarons having a spin $S = 1/2$, which gives a g-value around 2. Additionally, the low-temperature ESR measurements in Figure 2c,d, provide experimental confirmation of the presence of the predicted polaron pairs in the triplet state having a spin $S = 1$.[1,19] As mentioned above, absorption between 700 and 900 nm and in the NIR region, both correspond to polaronic/bipolaronic states, which is in line with the UV−vis−NIR and ESR results presented. Together, these results help to consolidate the revised interpretation of the UV−vis−NIR spectrum of PEDOT.

Similarly, based on the results obtained from the DFT calculated BLA of PEDOT as the charge increases in Figure 5, we propose a revised interpretation of the Raman spectrum of PEDOT. The intention here is that it will help to clarify the common misconception of the origin of the shifts of the vibrational modes of PEDOT proposed in 1999[55] that is still commonly found in recent articles.[56−58] The results presented in Figure 5 do not agree with the common conclusion that the complete conformational change between quinoidal and benzoidal conformations causes the Raman shifts. Instead, they should be discussed in terms of ED. It is possible to estimate the number of different ECLs present in the samples by performing a deconvolution of the main C_α=C_β symmetric stretching band. When PEDOT:PSS was post-treated with concentrations of HZ greater than 0.4 M (Table S2), the number of different ECL contributions is reduced from 5 to 4 with an accompanying reduction of their fwhm, indicating that there is a simultaneous ordering of the adjacent PEDOT chains as the ED is increased. This is accompanied by a change in the relative intensity of the main contributions to the C_α=C_β symmetric stretching band as the concentration of HZ is increased, where the dominant deconvoluted peak shifts from ∼1424 cm^{-1} for pristine PEDOT:PSS to ∼1406 cm^{-1} for the highest concentration of HZ, giving further indication of the growth of the ED.

In the case of the H_2SO_4 post-treated samples, the observed changes in Raman deconvolution follow the opposite trend. As the concentration of H_2SO_4 increases, there is an increase in the number of contributions corresponding to different ECLs, and they tend to shift to higher frequencies, indicating a shortening of the ED. Furthermore, as the number of different ECLs increases, there is a concomitant increase in the fwhm of the main contribution, suggesting a disruption of the ordering of adjacent PEDOT chains. Together, the combination of the theoretical and experimental results obtained from the BLA and deconvolution of the Raman spectra, respectively, support a revised interpretation of the vibrational shifts in Raman spectra for PEDOT with different oxidation levels.

From the results presented in Figure 6a, it can be found that there is only a small change in the σ values for samples post-treated with concentrations higher than 0.4 M HZ. This result is surprising since HZ is a strong reducing agent, and it has been reported to greatly reduce the σ of PEDOT:PSS.[30] To better understand the changes observed in the σ of PEDOT:PSS, a combination of ESR and σ measurements is necessary. As seen in Figure 2a, the modulation of the polaron concentration does not follow the expected trend where the polaron concentration gets periodically reduced with increasing concentration of HZ. Additionally, Figure 2c shows that the samples post-treated with HZ give rise to the signal corresponding to polaron pairs having a spin $S = 1$. Zozoulenko at el. demonstrated that polarons and bipolarons present very similar band structures, charge localization, and wave functions, suggesting that the features of electron transport are the same for polarons and bipolarons, and both contribute to the overall σ.[1] These results help to explain the observed trend in the variation and stabilization of the σ of PEDOT:PSS post-treated with different concentrations of HZ. As depicted in Figure 6b, there is a noticeable increase in the σ

https://doi.org/10.1021/acs.jpcc.4c05602
J. Phys. Chem. C 2024, 128, 18612−18621

of the PEDOT:PSS samples as the concentration of H_2SO_4 increases. Similar to the HZ post-treated samples, all the measured H_2SO_4 samples present the $S = 1/2$ and $S = 1$ ESR signals, as shown in Figure 2b,d, respectively, where the increasing concentration of H_2SO_4 does not follow the expected transformation of polarons into bipolarons as the oxidation level of PEDOT is increased. These results further support the theory that both polarons and bipolarons contribute to the overall σ. Furthermore, we cannot exclude the possibility of removal of excess PSS and the formation of PEDOT-rich crystalline nanofibers by H_2SO_4 post-treatments, contributing to the increase of the σ of PEDOT.[59] As pointed out by Zozoulenko et al., the interpretation of transport experiments that attribute different transport behaviors to differences in the nature of the charge carriers (polarons vs bipolarons) should be revisited.[1,60]

CONCLUSIONS

By analyzing the variations observed in the UV−vis−NIR spectra of PEDOT:PSS in conjunction with the ESR results, it was possible to corroborate and validate the proposed revised interpretation of the UV−vis−NIR spectrum postulated by Zozoulenko et al.[1] Additionally, low-temperature ESR measurements provided the first experimental evidence of the presence of polaron pairs in the triplet state (g-value > 2) in PEDOT:PSS, having a spin $S = 1$, which previously were only predicted theoretically. Furthermore, based on the results from the calculated BLA, we presented a revised interpretation of the shifts observed in the Raman spectra of PEDOT:PSS with varying oxidation levels. The proposed interpretation is accompanied by an experimental methodology that facilitates the analysis and evaluation of the different ECLs that are directly related to the ED in the oligomers.

Additionally, the σ measurements showed that even after post-treating PEDOT:PSS with increasing concentrations of HZ up to 1 M, the samples remained conductive, and it was possible to detect the presence of polarons and bipolarons. On the other hand, the H_2SO_4 post-treatment promotes an increase in the σ as the concentration of H_2SO_4 increases. Nevertheless, all samples showed the presence of polarons and bipolarons, and these results do not follow the "traditional" interpretation that there is a concomitant transformation of polarons into bipolarons, causing a decrease of the ESR signal as the oxidation level of PEDOT increases. Together, these results showcase that the features of electron transport of polarons and bipolarons are similar in PEDOT and that both contribute to the overall σ. Consequently, the notion that CPs composed of a bipolaron network (semimetallic) have better conduction properties than those with a polaron network (metallic) needs to be revisited.

This work provides valuable insights into the modulation of polarons and bipolarons present in PEDOT:PSS and presents a combination of theoretical and experimental methodologies that will help to better characterize the changes observed in the UV−vis−NIR spectroscopy, ESR spectroscopy, Raman spectroscopy, and σ measurements. These results underscore the importance of integrating theoretical and experimental analytical techniques that allow us to gain a deeper understanding of PEDOT behavior, providing the opportunity to tailor its properties for a range of different applications. While this study focuses on PEDOT, these strategies are relevant to various communities working with different CPs and organic semiconductors.

ASSOCIATED CONTENT

Supporting Information

The Supporting Information is available free of charge at https://pubs.acs.org/doi/10.1021/acs.jpcc.4c05602.

Calculated g-values for the HZ and H_2SO_4 post-treated PEDOT:PSS samples; deconvoluted Raman spectra of HZ and H_2SO_4 post-treated PEDOT:PSS samples; fitting parameters of the deconvoluted contributions of the symmetric C_α=C_β Raman signal of PEDOT:PSS samples; simulated Raman spectra of PEDOT with increasing net charge; conductivity measurements of pristine and HZ and H_2SO_4 post-treated PEDOT:PSS samples; conductivity error calculation; optical image of the measuring TFA chip (PDF)

AUTHOR INFORMATION

Corresponding Author

Katherine A. Mazzio − *Helmholtz-Zentrum Berlin für Materialien und Energie GmbH, 14109 Berlin, Germany; Institut für Chemie, Humboldt-Universität zu Berlin, 12489 Berlin, Germany;* orcid.org/0000-0001-9565-7301; Email: katherine.mazzio@helmholtz-berlin.de

Authors

Rodrigo Rubio-Govea − *Helmholtz-Zentrum Berlin für Materialien und Energie GmbH, 14109 Berlin, Germany; Institut für Chemie, Humboldt-Universität zu Berlin, 12489 Berlin, Germany;* orcid.org/0000-0001-7801-6254

Amanda Opis-Basilio − *Institut für Chemie, Humboldt-Universität zu Berlin, 12489 Berlin, Germany*

Adalid Torres − *Centro de Investigación en Materiales Avanzados, S.C. (Cimav), Subsede Monterrey, Apodaca, Nuevo León CP 66628, México*

Mario Sánchez − *Centro de Investigación en Materiales Avanzados, S.C. (Cimav), Subsede Monterrey, Apodaca, Nuevo León CP 66628, México*

Kallol Ray − *Institut für Chemie, Humboldt-Universität zu Berlin, 12489 Berlin, Germany;* orcid.org/0000-0003-2074-8844

Complete contact information is available at: https://pubs.acs.org/10.1021/acs.jpcc.4c05602

Notes

The authors declare no competing financial interest.

ACKNOWLEDGMENTS

This work was partially funded by the Deutsche Forschungsgemeinschaft (DFG, German Research Foundation) under Germany's Excellence Strategy—EXC 2008-390540038—UniSysCat to K.R; and A.O.B. thanks Einstein Foundation Berlin (ESB)—Einstein Center of Catalysis (EC^2) for their scholarship and support. This research was partially financed by CONAHCYT, who also kindly provided the Ph.D. scholarship to A.A. through the scholarship number: 2022-000018-02NACF-16100. We recognize Rodrigo Domínguez García for his professional technical support in using the supercomputing cluster prometeo.cimav.edu.mx.

REFERENCES

(1) Zozoulenko, I.; Singh, A.; Singh, S. K.; Gueskine, V.; Crispin, X.; Berggren, M. Polarons, Bipolarons, And Absorption Spectroscopy of PEDOT. *ACS Appl. Polym. Mater.* **2019**, *1* (1), 83−94.

(2) Chakraborty, A.; DiFilippo, A.; Deivasigamani, S.; Hong, C.; Madwesh, A.; Orlowski, M. Exploring Novel Methods: Acid Treatment, Metal Nanoparticle Doping, and Graphene Insertion for Enhanced Electrical Conductivity of Nm Thin PEDOT:PSS Films. *Synth. Met.* **2024**, *307*, No. 117694.
(3) Nie, S.; Qin, F.; Liu, Y.; Qiu, C.; Jin, Y.; Wang, H.; Liu, L.; Hu, L.; Su, Z.; Song, J.; et al. High Conductivity, Semiconducting, and Metallic PEDOT:PSS Electrode for All-Plastic Solar Cells. *Molecules* **2023**, *28* (6), 2836.
(4) Su, Z.; Jin, Y.; Wang, H.; Li, Z.; Huang, L.; Wang, H. PEDOT:PSS and Its Composites for Flexible Supercapacitors. *ACS Appl. Energy Mater.* **2022**, *5* (10), 11915−11932.
(5) Xu, H.; Zhao, X.; Yang, G.; Ji, X.; Zhang, X.; Li, L.; Wu, B.; Ouyang, X.; Ni, Y.; Chen, L.; et al. Modification of PEDOT:PSS towards High-Efficiency OLED Electrode via Synergistic Effect of Carboxy and Phenol Groups from Biomass Derivatives. *Chem. Eng. J.* **2022**, *430*, No. 133014.
(6) Nguyen-Dang, T.; Chae, S.; Harrison, K.; Llanes, L. C.; Yi, A.; Kim, H. J.; Biswas, S.; Visell, Y.; Bazan, G. C.; Nguyen, T.-Q. Efficient Fabrication of Organic Electrochemical Transistors via Wet Chemical Processing. *ACS Appl. Mater. Interfaces* **2022**, *14* (10), 12469−12478.
(7) Mazzio, K. A.; Kojda, D.; Rubio-Govea, R.; Niederhausen, J.; Ryll, B.; Raja-Thulasimani, M.; Habicht, K.; Raoux, S. P-Type-to-N-Type Transition in Hybrid Ag_xTe/PEDOT:PSS Thermoelectric Materials via Stoichiometric Control during Solution-Based Synthesis. *ACS Appl. Energy Mater.* **2020**, *3* (11), 10734−10743.
(8) Xu, Z.; Song, J.; Liu, B.; Lv, S.; Gao, F.; Luo, X.; Wang, P. A Conducting Polymer PEDOT:PSS Hydrogel Based Wearable Sensor for Accurate Uric Acid Detection in Human Sweat. *Sensors Actuators B Chem.* **2021**, *348*, No. 130674.
(9) Mo, Y.; Guo, J.; Liu, P.; Zeng, Q.; Chen, J.; Guo, C.; Deng, X.; Wang, W.; Li, G. Improved Photovoltaic Performance of GaAs/Carbon Nanotube Heterojunction Solar Cells with a Multifunctional Nafion/PEDOT:PSS Layer. *ACS Appl. Nano Mater.* **2023**, *6* (17), 15588−15596.
(10) Zozoulenko, I.; Franco-Gonzalez, J. F.; Gueskine, V.; Mehandzhiyski, A.; Modarresi, M.; Rolland, N.; Tybrandt, K. Electronic, Optical, Morphological, Transport, and Electrochemical Properties of PEDOT: A Theoretical Perspective. *Macromolecules* **2021**, *54* (13), 5915−5934.
(11) Almeida, P.; Izumi, C.; Santos, H.; Sant'Ana, A. C. Spectroscopic Characterization of PEDOT:PSS Conducting Polymer by Resonance Raman and SERRS Spectroscopies. *Quim. Nova* **2019**, *42* (9), 1073−1080.
(12) Mosca, S.; Milani, A.; Castiglioni, C.; Hernández Jolín, V.; Meseguer, C.; López Navarrete, J. T.; Zhao, C.; Sugiyasu, K.; Ruiz Delgado, M. C. Raman Fingerprints of π-Electron Delocalization in Polythiophene-Based Insulated Molecular Wires. *Macromolecules* **2022**, *55* (9), 3458−3468.
(13) Castiglioni, C.; Lopez Navarrete, J. T.; Zerbi, G.; Gussoni, M. A Simple Interpretation of the Vibrational Spectra of Undoped, Doped and Photoexcited Polyacetylene: Amplitude Mode Theory in the GF Formalism. *Solid State Commun.* **1988**, *65* (7), 625−630.
(14) Castiglioni, C.; Tommasini, M.; Zerbi, G. Raman Spectroscopy of Polyconjugated Molecules and Materials: Confinement Effect in One and Two Dimensions. *Philos. Trans. R. Soc. London. Ser. A Math. Phys. Eng. Sci.* **2004**, *362* (1824), 2425−2459.
(15) Ortiz, R. P.; Casado, J.; González, S. R.; Hernández, V.; Navarrete, J. T. L.; Viruela, P. M.; Ortí, E.; Takimiya, K.; Otsubo, T. Quinoidal Oligothiophenes: Towards Biradical Ground-State Species. *Chem. - Eur. J.* **2010**, *16* (2), 470−484.
(16) Burrezo, P. M.; Zafra, J. L.; López Navarrete, J. T.; Casado, J. Quinoidal/Aromatic Transformations in Π-Conjugated Oligomers: Vibrational Raman Studies on the Limits of Rupture for Π-Bonds. *Angew. Chemie Int. Ed.* **2017**, *56* (9), 2250−2259.
(17) Ferrón, C. C.; Sheynin, Y.; Li, M.; Patra, A.; Bendikov, M.; López Navarrete, J. T.; Hernández, V.; Ruiz Delgado, M. C. Raman Spectroscopic Characterization of Polyselenophenes and Poly(3,4-ethylenenedioxyselenophene)S. *Isr. J. Chem.* **2014**, *54* (5−6), 759−766.
(18) Casado, J.; Hernández, V.; López Navarrete, J. T. Vibrational Raman Shifts and Aromaticity: The Case of Oligothiophenes. *Chem. Rec.* **2015**, *15* (6), 1110−1118.
(19) Sahalianov, I.; Hynynen, J.; Barlow, S.; Marder, S. R.; Müller, C.; Zozoulenko, I. UV-to-IR Absorption of Molecularly p-Doped Polythiophenes with Alkyl and Oligoether Side Chains: Experiment and Interpretation Based on Density Functional Theory. *J. Phys. Chem. B* **2020**, *124* (49), 11280−11293.
(20) Karafiloglou, P. The Double (or Dynamic) Spin Polarization in π Diradicals. *J. Chem. Educ.* **1989**, *66* (10), 816.
(21) Tsoi, W. C.; James, D. T.; Kim, J. S.; Nicholson, P. G.; Murphy, C. E.; Bradley, D. D. C.; Nelson, J.; Kim, J.-S. The Nature of In-Plane Skeleton Raman Modes of P3HT and Their Correlation to the Degree of Molecular Order in P3HT:PCBM Blend Thin Films. *J. Am. Chem. Soc.* **2011**, *133* (25), 9834−9843.
(22) Linseis, V.; Völklein, F.; Reith, H.; Woias, P.; Nielsch, K. Platform for In-Plane ZT Measurement and Hall Coefficient Determination of Thin Films in a Temperature Range from 120 K up to 450 K. *J. Mater. Res.* **2016**, *31*, 3196−3204.
(23) Linseis, V.; Hassan, Z. M.; Reith, H.; Garcia, J.; Nielsch, K.; Baumgart, H.; Redel, E.; Woias, P. Complete Thermoelectric Characterization of PEDOT:PSS Thin Films with a Novel ZT Test Chip Platform. *Phys. Status Solidi A* **2018**, *215*, 1700930.
(24) Frisch, M. J.; Trucks, G. W.; Schlegel, H. B.; Scuseria, G. E.; Robb, M. A.; Cheeseman, J. R.; Scalmani, G.; Barone, V.; Petersson, G. A.; Nakatsuji, H.et al.*G16_C01. Gaussian 16*, Revision C.01, 2016; p Gaussian, Inc.: Wallin.
(25) Chai, J. Da; Head-Gordon, M. Long-Range Corrected Hybrid Density Functionals with Damped Atom−Atom Dispersion Corrections. *Phys. Chem. Chem. Phys.* **2008**, *10* (44), 6615−6620.
(26) Ditchfield, R.; Hehre, W. J.; Pople, J. A. Self-Consistent Molecular-Orbital Methods. IX. An Extended Gaussian-Type Basis for Molecular-Orbital Studies of Organic Molecules. *J. Chem. Phys.* **1971**, *54* (2), 724−728.
(27) Michaels, W.; Zhao, Y.; Qin, J. Atomistic Modeling of PEDOT:PSS Complexes I: DFT Benchmarking. *Macromolecules* **2021**, *54* (8), 3634−3646.
(28) Bubnova, O.; Crispin, X. Towards Polymer-Based Organic Thermoelectric Generators. *Energy Environ. Sci.* **2012**, *5* (11), 9345.
(29) Massonnet, N.; Carella, A.; Jaudouin, O.; Rannou, P.; Laval, G.; Celle, C.; Simonato, J.-P. Improvement of the Seebeck Coefficient of PEDOT:PSS by Chemical Reduction Combined with a Novel Method for Its Transfer Using Free-Standing Thin Films. *J. Mater. Chem. C* **2014**, *2* (7), 1278−1283.
(30) Yemata, T. A.; Zheng, Y.; Kyaw, A. K. K.; Wang, X.; Song, J.; Chin, W. S.; Xu, J. Modulation of the Doping Level of PEDOT:PSS Film by Treatment with Hydrazine to Improve the Seebeck Coefficient. *RSC Adv.* **2020**, *10* (3), 1786−1792.
(31) Zhang, L.; Yang, K.; Chen, R.; Zhou, Y.; Chen, S.; Zheng, Y.; Li, M.; Xu, C.; Tang, X.; Zang, Z.; et al. The Role of Mineral Acid Doping of PEDOT:PSS and Its Application in Organic Photovoltaics. *Adv. Electron. Mater.* **2020**, *6* (1), 1900648.
(32) Lee, J.-K.; You, S.; Jeon, S.; Ryu, N.-H.; Park, K. H.; Myung-Hoon, K.; Kim, D. H.; Kim, S. H.; Schiff, E. A. Electron Spin Resonance and Electrical Transport in Films of Poly (3,4-Ethylenedioxythiophene) Doped with Poly(Styrenesulphonate). *J. Appl. Phys.* **2015**, *118* (1), No. 015501.
(33) Serrano-Claumarchirant, J. F.; Culebras, M.; Muñoz-Espí, R.; Cantarero, A.; Gómez, C. M.; Collins, M. N. PEDOT Thin Films with N-Type Thermopower. *ACS Appl. Energy Mater.* **2020**, *3* (1), 861−867.
(34) Fu, Q.; Li, Y.; Wang, X.; Li, Q.; Wang, F.; Yang, R. The Importance of the Molecular Weight of PEDOT Hole Transporting Materials for Efficient Organic Solar Cells. *J. Mater. Chem. C* **2020**, *8* (48), 17185−17193.
(35) Li, Y.; Li, Q.; Wang, X.; Fu, Q.; Hu, C.; Qiu, X.; Li, T.; Wang, F. Eliminating the Detrimental Effect of Secondary Doping on

https://doi.org/10.1021/acs.jpcc.4c05602
J. Phys. Chem. C 2024, 128, 18612−18621

PEDOT: PSS Hole Transporting Material Performance. *ChemSusChem* **2021**, *14* (21), 4802−4811.
(36) Zykwinska, A.; Domagala, W.; Czardybon, A.; Pilawa, B.; Lapkowski, M. In Situ EPR Spectroelectrochemical Studies of Paramagnetic Centres in Poly(3,4-Ethylenedioxythiophene) (PEDOT) and Poly(3,4-Butylenedioxythiophene) (PBuDOT) Films. *Chem. Phys.* **2003**, *292* (1), 31−45.
(37) Eaton, G. R.; Eaton, S. S.; Barr, D. P.; Weber, R. T. Temperature. In *Quantitative EPR*; Springer Vienna: Vienna, 2010; pp 91−99. .
(38) Karunakaran, C.; Balamurugan, M. Chapter Four - Electron Paramagnetic Resonance Spectroscopy. In *Spin Resonance Spectroscopy: Principles and applications*; Karunakaran, C., Ed.; Elsevier, 2018; pp 169−228. .
(39) Casado, J.; Miller, L. L.; Mann, K. R.; Pappenfus, T. M.; Hernández, V.; López Navarrete, J. T. Experimental and Theoretical Study of the Infrared and Raman Spectra of a Substituted Sexithiophene in Five Oxidation States. *J. Phys. Chem. B* **2002**, *106* (14), 3597−3605.
(40) Casado, J.; Takimiya, K.; Otsubo, T.; Ramírez, F. J.; Quirante, J. J.; Ortiz, R. P.; González, S. R.; Oliva, M. M.; López Navarrete, J. T. Raman Spectroscopy Shows Interchain through Space Charge Delocalization in a Mixed Valence Oligothiophene Cation and in Its π-Dimeric Biradicaloid Dication. *J. Am. Chem. Soc.* **2008**, *130* (43), 14028−14029.
(41) Stavytska-Barba, M.; Kelley, A. M. Surface-Enhanced Raman Study of the Interaction of PEDOT:PSS with Plasmonically Active Nanoparticles. *J. Phys. Chem. C* **2010**, *114* (14), 6822−6830.
(42) Castro, C. M.; Delgado, M. C. R.; Hernández, V.; Hotta, S.; Casado, J.; López Navarrete, J. T. Efficiency of the π Conjugation in a Novel Family of α, α'-Bisphenyl End-Capped Oligothiophenes by Means of Raman Spectroscopy. *J. Chem. Phys.* **2002**, *116* (23), 10419−10427.
(43) González, S. R.; Ie, Y.; Aso, Y.; López Navarrete, J. T.; Casado, J. The Frontiers of Quinoidal Stability in Long Oligothiophenes: Raman Spectra of Dicationic Polaron Pairs. *J. Am. Chem. Soc.* **2011**, *133* (41), 16350−16353.
(44) Rubio-Govea, R.; Félix, R.; Wilks, R. G.; Bär, M.; Mazzio, K. A. Understanding the Effects of Primary and Secondary Doping via Post-Treatment of P-Type and N-Type Hybrid Organic−Inorganic Thin Film Thermoelectric Materials. *Adv. Electron. Mater.* **2023**, *9* (6), 2300076.
(45) Tran-Van, F.; Garreau, S.; Louarn, G.; Froyer, G.; Chevrot, C. A Fully Undoped Oligo(3,4-Ethylenedioxythiophene): Spectroscopic Properties. *Synth. Met.* **2001**, *119* (1−3), 381−382.
(46) Donohoo-Vallett, P. J.; Bragg, A. E. π-Delocalization and the Vibrational Spectroscopy of Conjugated Materials: Computational Insights on Raman Frequency Dispersion in Thiophene, Furan, and Pyrrole Oligomers. *J. Phys. Chem. B* **2015**, *119* (8), 3583−3594.
(47) Ouyang, J.; Xu, Q.; Chu, C.-W.; Yang, Y.; Li, G.; Shinar, J. On the Mechanism of Conductivity Enhancement in Poly(3,4-Ethylenedioxythiophene):Poly(Styrene Sulfonate) Film through Solvent Treatment. *Polymer (Guildf).* **2004**, *45* (25), 8443−8450.
(48) Xia, Y.; Zhang, H.; Ouyang, J. Highly Conductive PEDOT:PSS Films Prepared through a Treatment with Zwitterions and Their Application in Polymer Photovoltaic Cells. *J. Mater. Chem.* **2010**, *20* (43), 9740.
(49) Li, C.; Luo, D.; Wang, T.; Shan, C.; Li, C.; Sun, K.; Kyaw, A. K. K.; Ouyang, J. Great Enhancement in the Seebeck Coefficient and Thermoelectric Properties of Solid PEDOT:PSS Films Through Molecular Energy Filtering by Zwitterions. *Small Struct.* **2023**, *4* (11), 2300245.
(50) Yuan, X.; Zhang, G.; Peng, H.; Wang, J.; Wei, Q.; Wang, R.; Yang, Y. Structural Transformation of PEDOT on Si/PEDOT:PSS Hybrid Solar Cells by Doping Hydroquinone. *Energy Technol.* **2023**, *11* (11), 2300422.
(51) Duan, Z.; Phillips, J.; Liirò-Peluso, L.; Woodward, S.; Makarovsky, O.; Weir, M. P.; Pereira, H. J.; Amabilino, D. B. Conducting Poly(3,4-Ethylenedioxythiophene) Materials with Sustainable Carrageenan Counter-Ions and Their Thermoelectric Properties. *Mater. Adv.* **2023**, *4* (22), 5573−5584.
(52) IUPAC, Delocalization. In *The IUPAC Compendium of Chemical Terminology*; International Union of Pure and Applied Chemistry (IUPAC): Research Triangle Park, NC, 2006. .
(53) Jacquemin, D.; Adamo, C. Bond Length Alternation of Conjugated Oligomers: Wave Function and DFT Benchmarks. *J. Chem. Theory Comput.* **2011**, *7* (2), 369−376.
(54) Kim, D.; Zozoulenko, I. Why Is Pristine PEDOT Oxidized to 33%? A Density Functional Theory Study of Oxidative Polymerization Mechanism. *J. Phys. Chem. B* **2019**, *123* (24), 5160−5167.
(55) Garreau, S.; Louam, G.; Lefrant, S.; Buisson, J. P.; Froyer, G. Optical Study and Vibrational Analysis of the Poly (3,4-Ethylenedioxythiophene) (PEDT). *Synth. Met.* **1999**, *101* (1−3), 312−313.
(56) Liu, L.; Yang, H.; Zhang, Z.; Wang, Y.; Piao, J.; Dai, Y.; Cai, B.; Shen, W.; Cao, K.; Chen, S. Photopatternable and Highly Conductive PEDOT:PSS Electrodes for Flexible Perovskite Light-Emitting Diodes. *ACS Appl. Mater. Interfaces* **2023**, *15* (17), 21344−21353.
(57) Osazuwa, P. O.; Lo, C.-Y.; Feng, X.; Nolin, A.; Dhong, C.; Kayser, L. V. Surface Functionalization with (3-Glycidyloxypropyl)-Trimethoxysilane (GOPS) as an Alternative to Blending for Enhancing the Aqueous Stability and Electronic Performance of PEDOT:PSS Thin Films. *ACS Appl. Mater. Interfaces* **2023**, *15* (47), 54711−54720.
(58) Sharma, N.; Koshy, A. M.; Kandregula, G. R.; Ramanujam, K.; Ray, D.; Swaminathan, P. Printed Silver Nanowire-PEDOT:PSS Composite Electrodes for Flexible Transparent Microsupercapacitor Applications. *ACS Appl. Energy Mater.* **2024**, *7* (1), 363−372.
(59) Kim, N.; Kee, S.; Lee, S. H.; Lee, B. H.; Kahng, Y. H.; Jo, Y.-R.; Kim, B.-J.; Lee, K. Highly Conductive PEDOT:PSS Nanofibrils Induced by Solution-Processed Crystallization. *Adv. Mater.* **2014**, *26* (14), 2268−2272.
(60) Bubnova, O.; Khan, Z. U.; Wang, H.; Braun, S.; Evans, D. R.; Fabretto, M.; Hojati-Talemi, P.; Dagnelund, D.; Arlin, J.-B.; Geerts, Y. H.; et al. Semi-Metallic Polymers. *Nat. Mater.* **2014**, *13* (2), 190−194.

https://doi.org/10.1021/acs.jpcc.4c05602
J. Phys. Chem. C 2024, 128, 18612−18621